

Stress-induced self-organization of nanoscale structures in SiGe/Si multilayer films

C. Teichert and M. G. Lagally
University of Wisconsin–Madison, Madison, Wisconsin 53706

L. J. Peticolas and J. C. Bean
AT&T Bell Laboratories, Murray Hill, New Jersey 07974

J. Tersoff
IBM Thomas J. Watson Research Center, Yorktown Heights, New York 10598
 (Received 14 February 1996)

In the growth of $\text{Si}_{1-x}\text{Ge}_x$ films on Si(001), the growth front undergoes a series of elastic stress relief mechanisms. We use these mechanisms in the molecular-beam-epitaxy growth of SiGe/Si superlattices to create relatively periodic surface and interface patterns of small coherent {105}-faceted SiGe crystallites. The self-organization of these islands is affected in different ways by tuning substrate miscut, alloy composition, and layer thickness. [S0163-1829(96)07423-1]

Spatial self-organization within particle ensembles is a common phenomenon in nature, covering a wide range of length scales and leading to beautiful patterns such as snowflakes, ripples on dunes, and cloud structures. Recently, scanned-probe methods have made possible direct access to this phenomenon on the nanometer and subnanometer scale. Surface reconstruction and pattern formation in homoepitaxial growth are self-organization processes on an atomic scale, driven by the system's desire to reduce its chemical free energy. In heteroepitaxy the relief of the built-up stress can be additional driving force for self-organization. Stress generally causes morphological changes at a scale larger than that due to chemical forces, such as one-dimensional (1D) ripple formation due to bunching of atomic-height steps^{1–3} and the formation of faceted 3D crystallites.^{4–6} Creating conditions favorable for the self-organization of such morphological features into ordered arrays on solid surfaces may become an elegant way to fabricate nanoscale structures⁷ that may meet the demands of miniaturization in high-technology applications, for example, in chip-to-chip communication.⁸

We show in this paper that stress-driven self-organization of very small crystallites in SiGe/Si multilayer films yields highly organized nanoscale structures. On a single layer of SiGe alloy, small crystals, formed in the shape of prismatic “huts” with {105} facets and coherent with the substrate,⁴ exhibit a broad distribution in size and shape. In a multilayer (consisting of alternate layers of pure Si and SiGe alloy) grown at the proper conditions, they organize into uniformly sized crystals in a square pattern. The self-organization is mediated by the presence of the Si spacer layers. Because we can control the thickness of these layers, we can control the process of self-organization. Substrate miscut further influences the organization.

Device-quality $\text{Si}_{1-x}\text{Ge}_x/\text{Si}$ superlattices were grown by molecular-beam epitaxy at 550 °C on vicinal Si(001) wafers. The polar and azimuthal miscut angles of the substrate, θ and ϕ , respectively, as well as the Ge concentration x in the alloy layers, were measured directly using x-ray diffraction.²

After depositing a 100-nm Si buffer layer up to 40 bilayers were grown at a deposition rate of 0.055 nm/s. If not otherwise specified, the individual layer thicknesses were 2.5 nm for the alloy layers and 10 nm for the Si spacer layers. The growth front morphology was investigated using *ex situ* atomic-force microscopy (AFM), in contact mode with a 12- μm xyz scanner. Conventional cantilevers with silicon nitride tips with a 70° side wall profile and a tip radius ranging between 20 and 40 nm were used.

Figure 1 shows AFM images of the surface of (a) a single layer of $\text{Si}_{0.25}\text{Ge}_{0.75}$ alloy film and (c) the 20th alloy layer of a $\text{Si}_{0.25}\text{Ge}_{0.75}\text{Si}$ multilayer film that were grown on a substrate with miscuts of $\theta=0.25^\circ$ and $\phi=25^\circ$ with respect to $[\bar{1}10]$. Both surfaces show 3D SiGe crystals (conventionally and hereafter called “islands”) with the edges of their bases parallel to the [100] or [010] directions. For a single alloy layer [Fig. 1(a)] these islands have mostly rectangular bases with an elongation in either the [100] or the [010] direction. They are arbitrarily arranged in an interlocked array, with a broad size distribution. A line scan analysis along these directions reveals that the side slopes of the islands are tilted with respect to the (001) plane by $11^\circ \pm 3^\circ$; i.e., these islands are bounded by {105} facets and are thus the “hut” clusters found earlier.^{4,5} Even though it is not evident from the images, the line scans confirm that the “huts” are touching each other.

With increasing bilayer number, the islands exhibit a degree of self-organization: they become larger, they adopt more or less square bases, and they arrange preferentially on chains along $\langle 100 \rangle$ or even on a square pattern [Fig. 1(c)]. The self-assembly can be quantified by analyzing the power spectral density of the surface roughness.⁹ Along with each image in Fig. 1 we show the two-dimensional power spectrum. These spectra exhibit clear fourfold patterns. For a single alloy layer, the pattern is broad and framelike [Fig. 1(b)]; with increasing bilayer number it converts into four relatively sharp peaks with corresponding higher orders [Fig. 1(d)]. This transformation indicates an increase of uniformity in size and shape of the islands.

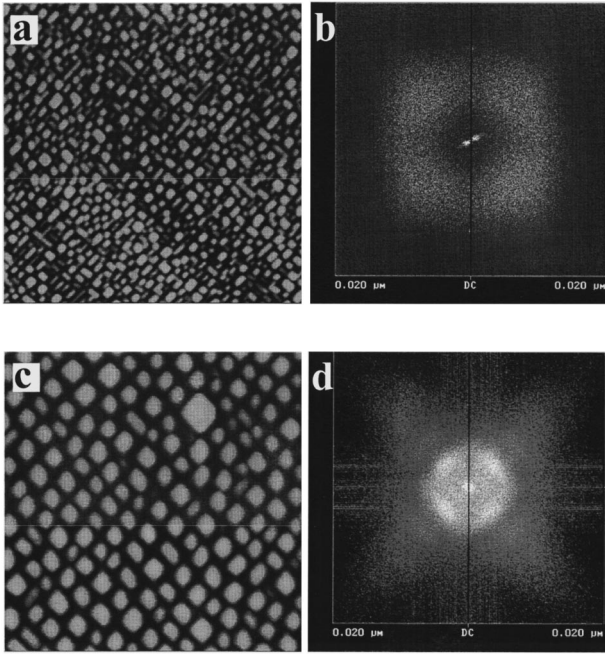


FIG. 1. AFM images of SiGe alloy-terminated surfaces of SiGe/Si multilayer films and the corresponding 2D power spectra. The horizontal direction is [110]. (a),(b) 25-Å $\text{Si}_{0.25}\text{Ge}_{0.75}$ single layer; (c),(d) $20\times$ (25-Å $\text{Si}_{0.25}\text{Ge}_{0.75}$ /100-Å Si) multilayer film. The gray-scale range of the real-space images is (a) 5 nm and (c) 20 nm, the image size is $1\ \mu\text{m}\times 1\ \mu\text{m}$. The 2D power spectra, ranging from -50 to $50\ \mu\text{m}^{-1}$, have been calculated from $5\ \mu\text{m}\times 5\ \mu\text{m}$ images. The faintly visible bright and dark bands extending from approximately upper left to lower right in (a) are step-bunched ripples with a wavelength of ~ 600 nm. The split peak in the center of the power spectrum in (b) reflects the orientation (25°) and periodicity of these ripples.

The predominant island spacing along $\langle 100 \rangle$ (and equivalently the base size, since the clusters touch each other) and the island size distribution can be obtained from the peak position and the peak width in a cut through the 2D power spectrum along that direction. Figure 2 shows power spectra for the first and the 20th alloy layers. The narrowing of the full width at half maximum of the peak indicates improved ordering. Figure 3 summarizes the results for a series of bilayer numbers. It shows the evolution of (a) the mean island spacing $\langle l \rangle$ and the width of the size distribution $\Delta l / \langle l \rangle$ and (b) the average aspect ratio of the island bases. The mean length of the island base increases with increasing bilayer number from ~ 35 nm for a single layer and approaches a stationary value of ~ 100 nm. The width of the size distribution relative to the average island size decreases from 1.1 for the first layer to 0.3 for 20 bilayers. This narrowing of the size distribution is clear evidence for a self-organization process. The evolution of the average aspect ratio of the island bases [Fig. 3(b)], decreasing from 1.5 for a single alloy layer to 1.15 for 40 bilayers, indicates a change in crystal shape from prismatic hut to approximately a four-sided pyramid. The island height changes from ~ 3 to ~ 10 nm. Using the measured dimensions, we can estimate the volume of the islands. The mean volume of islands on a

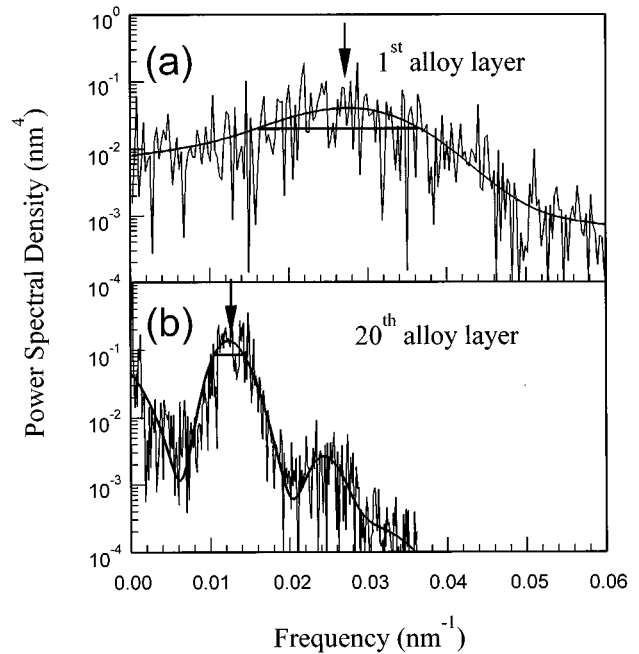


FIG. 2. Cuts along [010] through the 2D power spectra shown in Fig. 1 for (a) the first alloy layer and (b) the 20th layer along with spline fits. The location of the peaks (arrows) yields the mean island separation along [010]. The full width of half maximum (horizontal lines) gives the width of the island size distribution.

single layer is about $1300\ \text{nm}^3$, consisting of 3.2×10^4 atoms, but with a wide distribution. At the limit of 40 bilayers for this set of parameters, the volume of the predominant-size island is about $3.6\times 10^4\ \text{nm}^3$, containing about 9×10^5 atoms.

The Si spacer layer influences the growth front morphology and the self-organization. It is known that pure Si deposited on top of the alloy layer smooths out the island morphology.^{10,11} Here the 10-nm Si spacer layer was sufficient to smooth the growth front to nearly what it was for the substrate. If we increase the Si spacer thickness to 300 nm at conditions otherwise identical to those of the 20-bilayer film shown in Fig. 1(c) we observe a much less pronounced self-organization. Without the interspersal of Si spacer layers, the self-organization does not occur at all: a 50-nm-thick single $\text{Si}_{0.25}\text{Ge}_{0.75}$ film [corresponding to the total SiGe alloy content of the multilayer film shown in Fig. 1(c), but without the Si spacer layers] exhibits randomly arranged, irregularly shaped large clusters mostly bounded by the steeper {113} and {158} facets.⁶ Hence the Si spacer layers act as a control on the self-organization.

We have shown elsewhere^{2,3} that under appropriate conditions of alloy composition and substrate miscut, an earlier stage of stress relief is the step bunching of preexisting substrate steps. This step bunching produces a rippled morphology, in which the up and down slopes of the ripples consist of an extended (001) terrace and an equal-sized area of high step density. For a given deposition rate, the spacing and orientation of the ripples can be tuned by varying the polar and azimuthal miscut angles of the substrate.¹² A careful

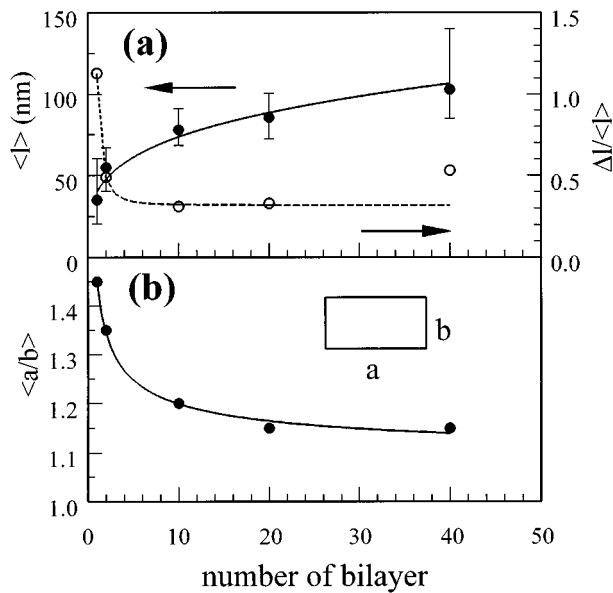


FIG. 3. Evolution of characteristic island parameters and surface roughness of 25-Å Si_{0.25}Ge_{0.75}/100-Å Si films as a function of the number of bilayers. The lines are guides to the eye. (a) Mean island spacing $\langle l \rangle$ along $\langle 100 \rangle$ (solid line) and relative width of the distribution, $\Delta l / \langle l \rangle$ (dashed line). The error bars indicate the width of the distribution of island spacings. The high data point in $\Delta l / \langle l \rangle$ at 40 bilayers is caused by the existence of a few large, no longer coherent clusters (Ref. 6) that also distort the size distribution (error bar in $\langle l \rangle$). The onset of formation of these clusters can be avoided by modifying the alloy composition or alloy layer thickness. (b) Average aspect ratio of the cluster bases, $\langle a/b \rangle$ (see inset).

look at Fig. 1(a) shows these ripples as bright and dark bands that extend from approximately upper left to lower right with an orientation that is 25° off the $[\bar{1}10]$ direction (in agreement with the azimuthal miscut angle). From the corresponding twofold low-frequency feature in the power spectrum [see the split central spot in Fig. 1(b)] an average ripple distance of 600 nm is determined. The coherent 3D SiGe islands, which represent a later stage of strain relief, are superimposed on that ripple structure. For proper orientation and spacing of the ripples an influence on the ordering of the islands is achievable. For example, Si(001) miscut by 2° produces a 1D ripple pattern with a periodicity of ~70 nm as the substrate steps bunch in the deposited film.^{2,3} For alloy layers with low ($\leq 50\%$) Ge concentration, only the ripples form at these deposition conditions. For alloy layers with higher Ge concentration, coherent islands of the “hut” type form and can be guided by the ripples. A very clear influence is observed if the substrate is miscut toward $\langle 100 \rangle$. Because the ripple direction is always determined by the substrate miscut, the ripples then also lie along $\langle 100 \rangle$. If an alloy layer with a high Ge concentration (e.g., $x=0.75$) is grown on a Si(001) substrate miscut 2° toward $\langle 100 \rangle$, the coherent 3D hut islands form in chains along the ripples (i.e., parallel to the $[010]$ direction). Effectively one of the two orientations of the elongated huts shown in Fig. 1(a) is eliminated. The 2D power spectrum reveals a high degree of order in size and

position of these “hut” islands, with very good ordering of the chains and additional ordering of the huts within each chain. Analysis of the spectrum yields a predominant base size of about 35×55 nm² with a very narrow distribution of the island width (35 ± 3.5 nm) and the island height (3 ± 0.3 nm). The lengths of the islands are more broadly distributed, reflecting less ordering within the chains. Because we can adjust the ripple wavelength by controlling the original substrate miscut, we expect that we can arbitrarily control at least the width (and therefore the height) of the 3D islands as well as obviously their organization into highly ordered chains. Combining the use of the Si spacer layer (whose thickness we can control), we expect that we can also control the regularity in size and spacing of the 3D islands along the chain.

How can we explain the observed self-organization? As we have seen above, it is clearly a property of the multilayer structure, i.e., it is mediated by the Si spacer layers. The spacer layer may act in principle either to copy the morphology of the surface on which it is deposited or to mediate the strain. The former can be ruled out because the deposition of a 10-nm Si layer smooths the growth front to the original substrate roughness, as we have pointed out. Therefore the Si spacer layer acts to create a strain distribution that is favorable for the formation of regularly spaced and sized islands. X-ray diffraction measurements on the same multilayers reveal a partially vertically correlated roughness in the multilayer.² Several other measurements of 3D islands in adjacent alloy layers located predominantly on top of each other have been reported.^{11,13–16} We have recently shown, within the framework of continuum elasticity theory,¹⁷ that the surface strain due to a buried cluster causes a preferential nucleation of a new cluster just above the buried one. The lateral interaction of these strain fields results in an increasingly regular cluster separation in successive layers; i.e., smaller and misaligned clusters are “thinned out” by the strain mediation through the Si spacer. The spacer layer acts as a bandpass filter for the morphology. The model explains the narrowing of the cluster size distribution and the increase of the average cluster size with increasing layer number observed in the experiment and predicts the observed dependence of the self-organization on the spacer layer thickness.

In conclusion, we have demonstrated ways to create regular SiGe nanoscale structures in SiGe/Si multilayer films through the self-organization of regular, coherent, prism-, or pyramid-shaped 3D SiGe islands that form to relieve stress. This self-organization occurs through the strain mediation by the Si spacer layers. The self-organization can be influenced by substrate miscut direction and magnitude (leading to alignment in chains) and by composition of the alloy layer as well as thickness of the spacer layer. The self-organization is understood in a simple model of interacting surface strain due to buried islands. We expect that one can produce a variety of similar and other nanoscale structural patterns in which there exist positional and size correlations not just in the surface plane but from layer to layer by exploiting knowledge of stress-relief mechanisms in multilayer films.

This work was supported by NSF Grant No. DMR92-01856. We would like to acknowledge helpful discussions with Y. H. Phang, D. E. Savage, and M. B. Webb, as well as technical assistance by K.-C. Liu and P.-F. Lam. We thank

P. Wagner, Wacker Siltronic GmbH, Burghausen, Germany for providing some of the wafers used here. C.T. acknowledges support from the German Academic Exchange Service.

-
- ¹M. Shinohara and N. Inoue, *Appl. Phys. Lett.* **66**, 1936 (1995).
- ²Y. H. Phang, Ch. Teichert, M. G. Lagally, L. Peticolas, J. C. Bean, and E. Kasper, *Phys. Rev. B* **50**, 14 435 (1994).
- ³J. Tersoff, Y. H. Phang, Z. Zhang, and M. G. Lagally, *Phys. Rev. Lett.* **75**, 2730 (1995).
- ⁴Y.-W. Mo, D. E. Savage, B. S. Swartzentruber, and M. G. Lagally, *Phys. Rev. Lett.* **65**, 1020 (1990).
- ⁵A. J. Pidduck, D. J. Robbins, A. G. Cullis, W. Y. Leong, and A. M. Pitt, *Thin Solid Films* **222**, 78 (1992).
- ⁶M. A. Lutz, R. M. Feenstra, P. M. Mooney, J. Tersoff, and J. O. Chu, *Surf. Sci.* **316**, L1075 (1994).
- ⁷R. Nötzel, T. Fukui, and H. Hasegawa, *J. Appl. Phys.* **65**, 2854 (1994); D. Leonard, M. Krishnamurthy, C. M. Reaves, S. P. Denbaars, and P. M. Petroff, *Appl. Phys. Lett.* **63**, 3203 (1993).
- ⁸H. Presting, H. Kibbel, M. Jaros, R. M. Turton, U. Menczigar, G. Abstreiter, and H. G. Grimmeiss, *Semicond. Sci. Technol.* **7**, 1127 (1992).
- ⁹See, e.g., J. M. Elson, H. E. Bennett, and J. M. Bennett, *Appl. Opt. Opt. Eng.* **69**, 191 (1979); H.-N. Yang, G.-C. Wang, and T.-M. Lu, *Diffraction from Rough Surfaces and Dynamic Growth Fronts* (World Scientific, Singapore, 1993), p. 64; W. M. Tong and R. S. Williams, *Annu. Rev. Phys. Chem.* **45**, 401 (1994).
- ¹⁰H. Sunamura, Y. Shiraki, and S. Fukatsu, *Appl. Phys. Lett.* **66**, 953 (1995).
- ¹¹T. S. Kuan and S. S. Iyer, *Appl. Phys. Lett.* **59**, 2242 (1991).
- ¹²C. Teichert, Y. H. Phang, L. J. Peticolas, J. C. Bean, and M. G. Lagally (unpublished).
- ¹³L. Goldstein, F. Glas, J. Y. Marzin, M. N. Charasse, and G. LeRoux, *Appl. Phys. Lett.* **47**, 1099 (1985).
- ¹⁴J. Y. Yao, T. G. Andersson, and G. L. Dunlop, *J. Appl. Phys.* **69**, 2224 (1991).
- ¹⁵L. Vescan, W. Jäger, C. Dieker, K. Schmidt, A. Hartman, and H. Lüth, in *Mechanisms of Heteroepitaxial Growth*, edited by M. F. Chisholm *et al.*, MRS Symposia Proceedings No. 263 (Materials Research Society, Pittsburgh, 1992), p. 23.
- ¹⁶Q. Xie, A. Madhukar, P. Chen, and N. P. Kobayashi, *Phys. Rev. Lett.* **75**, 2542 (1995).
- ¹⁷J. Tersoff, C. Teichert, and M. G. Lagally, *Phys. Rev. Lett.* **76**, 1675 (1996).